

Elastic Scattering of 5.6-Mev Neutrons from Carbon

J. E. BRALEY* AND C. W. COOK

Convair, San Diego, California

(Received October 26, 1959)

Energetic neutrons produced from the $D(d,n)He^3$ reaction have been scattered from a cylindrical carbon sample to study the angular distribution of elastically-scattered, 5.6-Mev neutrons. The differential elastic scattering cross sections for carbon have been obtained for angles in the range of 30 to 150 degrees. A thin plastic neutron-proton recoil detector was used in the measurements to permit discrimination against 4.4-Mev gamma rays from the carbon sample, and other gamma-ray backgrounds.

INTRODUCTION

MEASUREMENTS of angular distributions for the scattering of fast neutrons from elements have considerably advanced the understanding of neutron interactions with nuclei by providing experimental data to check the potential shapes and parameters of various nuclear models. The angular distribution data are not only of theoretical interest, but are also of considerable practical importance in reactor design and neutron shielding calculations.

Angular distribution measurements for elastically-scattered neutrons from carbon have been reported for a number of neutron energies in the million electron volt region.¹⁻⁴ However, since the distribution for light elements can not be predicted with the same degree of accuracy possible for heavier elements,⁵ further measurements are desirable in energy regions where rapid changes in the angular distributions with energy have been seen to occur. The measurement of the angular distribution of elastically-scattered, 5.6-Mev neutrons from carbon will be discussed.

EQUIPMENT AND EXPERIMENTAL PROCEDURE

The experimental arrangement is shown schematically in Fig. 1. A deuteron beam from a 3-Mev Van de Graaff accelerator⁶ bombarded a deuterium gas target to produce 5.6-Mev neutrons at an angle of 5 degrees with the forward direction. These neutrons were scattered by a 3.73-cm diam and 4.76-cm long cylindrical carbon⁷ sample. The angular distribution of elastically-scattered neutrons was measured with a biased scintillation counter. Multiple scattering of

neutrons in the sample was kept small by choosing the diameter of the carbon to be approximately one-third of a neutron mean free path. This choice of diameter introduced a neutron energy spread of approximately 25 kev caused by the finite angular extension of the sample as viewed from the neutron source. The choice of diameter results in about 18% of the initially scattered neutrons having more than one collision before leaving the sample, i.e., about 18% of the neutrons reaching the detector had been scattered at least twice.

The distance between the neutron source and scatterer was 29.6 cm, and the detector was placed 20.3 cm from the scatterer for all scattering measurements. An iron shield was placed between the neutron source and the detector to reduce the background emanating directly from the source. The shield consisted of removable sections which made measurements possible at 15-degree intervals between 30 and 150 degrees with respect to the incident neutrons. Neutron scattering from the shield accounted for 8% of the total flux at the sample position when the full shield was employed; considerably less neutron scattering was present in measurements taken for scattering angles which required only segments of the shield. For the 30-degree measurements, the background counting rate with the sample removed was about 70% of the counting rate with the sample in place. The background counting rate increased slightly with the scattering angle, except at the 153-degree position, where the background was unusually high.

The gas target chamber was 3.35 cm long and was separated from the accelerating tube vacuum system by a 3.26 mg/cm² nickel foil. The target pressure was maintained at 22 in. of mercury which caused a spread in the neutron energy of approximately ± 60 kev. Deuteron straggling in the nickel foil caused about a 16-kev spread in neutron energy. A deuterium beam current of less than about 1 μ a was used throughout the experiment to prolong the life of the nickel foil.

The neutron detector consisted of a single 2.7-cm diam, $\frac{1}{8}$ -in. thick Plastic B scintillator⁸ mounted on an RCA-6342 photomultiplier tube. A mu-metal cylinder

* Now at the University of California, Berkeley, California.

¹ *Neutron Cross Sections, Angular Distributions*, compiled by D. J. Hughes and R. S. Carter, Brookhaven National Laboratory Report BNL-400 (Office of Technical Services, U. S. Department of Commerce, Washington, D. C., 1956).

² J. R. Beyster, M. Walt, and E. W. Salmi, *Phys. Rev.* **104**, 1319 (1956); M. Walt and J. R. Beyster, *Phys. Rev.* **98**, 677 (1955).

³ J. E. Wills, J. K. Bair, H. O. Cohn, and H. B. Willard, *Phys. Rev.* **109**, 891 (1958).

⁴ R. W. Hill, *Phys. Rev.* **109**, 2105 (1958).

⁵ J. R. Beyster (private communication); F. E. Bjorklund (private communication).

⁶ Located at Lockheed Missile Systems Division, Palo Alto, California.

⁷ GSXP grade graphite obtained from Graphite Specialties Corporation, Niagara Falls, New York.

⁸ Obtained from the Pilot Chemical Company, Waltham, Massachusetts.

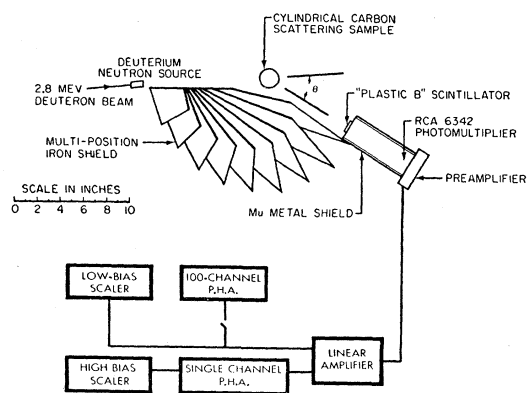


FIG. 1. Schematic (top view) of experimental arrangement.

was placed around the photomultiplier tube for magnetic shielding. The detector was thin enough so that pulses resulting from the 4.4-Mev gamma rays from C^{12} could be electronically biased out.

Scattering measurements were taken using two different bias settings simultaneously. A difference in the cross section resulting from the use of the different settings would indicate that the lower setting was not high enough to bias out pulses from the gamma-ray background or from inelastically-scattered neutrons.

One bias setting was not changed while the scattering measurements were taken; the other setting was varied because the momentum transfer to the target nucleus varies with the scattering angle. The relative efficiency of the counting system as a function of neutron energy for several bias settings is shown in Fig. 2. The different neutron energies used in obtaining Fig. 2 were obtained by placing the detector in the sample position and by changing the energy of the incident deuteron beam.

The differential scattering cross section, subject to several corrections, is given by the formula:

$$\sigma(\theta) = [(S-B)/D](R^2/N), \quad (1)$$

where S is the number of counts with the detector at angle θ and distance R from the scatterer for a given integrated charge of deuteron beam current incident on the target, B is the corresponding number of counts with the scatterer removed, D is the number of counts with the detector at the position normally occupied by the scatterer, and N is the number of nuclei in the scattering sample. At each angle, S and B were measured alternately, the sample being removed and replaced mechanically. The direct beam count was measured either before or after each series of runs with the appropriate shield configuration in place. All runs consisted of collecting the same integrated deuteron charge at the target and usually lasted about 65 sec. The S and B for each angle were corrected for differences in background counts caused by variations in the time required to collect the charge at the target. This correction to D was negligible. Cross-section measure-

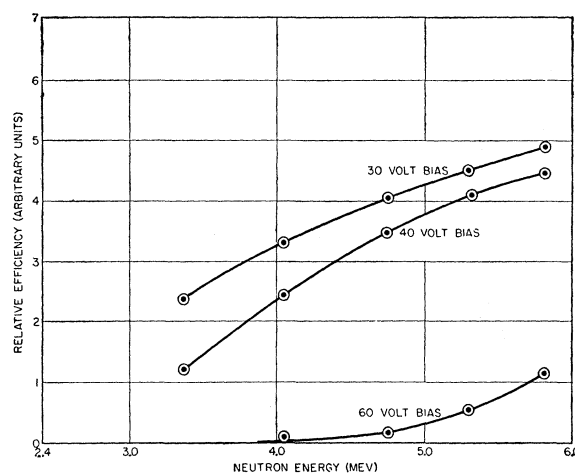


FIG. 2. Neutron energy vs relative efficiency.

ments were made at angles of 34.1, 48.6, 64.0, 78.5, 93.8, 108.5, 123.4, and 152.8 degrees. The angles were corrected for the finite length of the scatterer and are accurate to ± 2 degrees; the angular resolution of the system was ± 7 degrees.

ANALYSIS OF THE DATA

The cross sections computed from Eq. (1) were corrected for the difference in counter efficiency for the detection of primary and scattered neutrons, attenuation of the incident flux in the scatterer, and multiple scattering of neutrons in the scatterer. The counter efficiency for detection of primary and scattered neutrons differs since momentum transfer to the target nucleus reduces the energy of the scattered neutrons. The correction for this effect was made by calculating the loss in neutron energy at each scattering angle and by obtaining the ratio of the detector efficiency for neutrons of the primary and scattered energy from the data shown in Fig. 2.

The correction for multiple scattering was made by the Monte Carlo method. In this method the multiple scattering is calculated on an assumed angular distribution for elastic scattering. The process is repeated for different assumed distributions until the calculated cross section agrees with the experimental data. The calculation traced 80 000 neutrons through the scattering sample and recorded the number of scattered neutrons passing through a cylindrical counting band 20.3 cm in radius and 2.7 cm high in 5-degree intervals of the scattering angle θ . The counting band was coaxial with the scattering cylinder and simulated the actual geometry. The Monte Carlo calculation thus approximated the angular resolution of the experimental arrangement as well as the multiple scattering. The attenuation of the incident flux caused by elastic scattering within the scatterer is inherent in the Monte Carlo calculation and the value obtained in this manner

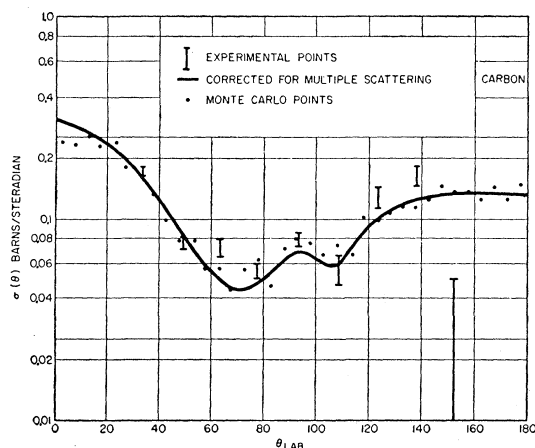


FIG. 3. Differential scattering cross section for 5.6-Mev neutrons.

was found to agree within 0.25% with that obtained analytically.⁹ The Monte Carlo problem was coded for the IBM-704 digital computer.

RESULTS

Figure 3 shows the experimental points corrected for counter efficiency and for the attenuation of incident neutrons in the sample. All quantities are given in the laboratory system of coordinates. The cross sections obtained from the data taken at the two bias settings were always in good agreement and thus indicate that significant amounts of inelastic neutron scattering or gamma rays were not present in the data obtained at the low bias settings. The experimental points shown are the averages of the cross-section values computed for the two bias settings. The solid line represents the input to the Monte Carlo calculation and thus is the fully corrected differential cross section for elastic scattering. The dots represent the Monte Carlo output and display the agreement with the experimental data. The experimental points carry the probable errors resulting from counting statistics only; the absolute values of the points are estimated to be accurate to about 20% with the exception of the point at 153 degrees, where counting statistics were very poor because of the extremely high background.

The inelastic collision cross section obtained by integrating the measured differential cross section for elastic scattering over 4π steradians and subtracting the result from the total cross section is in agreement with previous measurements^{2,10} of the inelastic cross section at other energies within the errors of the measurements.

⁹ M. Walt, Ph.D. thesis, University of Wisconsin, 1953 (unpublished). The cross section was obtained by integrating the elastic scattering data presented here.

¹⁰ M. H. MacGregor, W. P. Ball, and R. Booth, Phys. Rev. **108**, 726 (1957).

DISCUSSION

The general features of fast-neutron interactions with nuclei have been described¹¹⁻¹⁶ with considerable success in terms of an optical model of the nucleus. In this model, the nucleus is represented by a complex potential well. Explicit calculations made with this model yield σ_t , the total cross section; σ_e , the cross section for the formation of a compound nucleus; and $\sigma_{se}(\theta)$, the differential shape-elastic scattering cross section, i.e., that part of the elastic scattering cross section which is not associated with compound nucleus formation (hard sphere scattering). On the other hand, experimental measurements yield (1) σ_t ; (2) σ_{ne} , the non-elastic cross section; (3) $\sigma_{el}(\theta)$, the differential cross section for elastic scattering; and (4) $\sigma_{in}(\theta)$ the cross section for inelastic scattering, i.e., scattering that leaves the scattering nucleus in an excited state. The nonelastic cross section, σ_{ne} , is given by σ_e minus σ_{ee} where σ_{ee} is the cross section for compound elastic scattering (the elastic scattering produced by the decay of the compound nucleus through the entrance channel). The elastic scattering cross section, $\sigma_{el}(\theta)$, is given by the sum of $\sigma_{se}(\theta)$ and $\sigma_{ce}(\theta)$. Thus experimental and theoretical cross sections are not always directly comparable. However, if a compound nucleus has many levels available for its decay in the residual nucleus, competing modes of decay reduce the probability of compound-elastic scattering. In this case $\sigma_{ce}(\theta)$ approaches zero and $\sigma_{el}(\theta)$ may be compared with $\sigma_{se}(\theta)$. On the other hand, if the level spacings are quite large so that the influence of individual resonances may be great, this model, which assumes an average over many resonances in the continuum region, may not be applicable.

Several complex potential models are in use. Bjorklund and Fernbach¹⁵ employ a potential containing (a) a diffuse-boundary real central well (V_{CR}), (b) a Gaussian centered on the nuclear edge for the imaginary "central" well (V_{CI}), and (c) a spin-orbit term (V_{SR}):

$$V = V_{CR}\rho(r) + iV_{CI}q(r) + V_{SR}\left(\frac{\hbar}{\mu c}\right)^2 \frac{1}{r} \frac{d\rho(r)}{dr} \cdot \sigma \cdot \mathbf{l},$$

where

$$\rho(r) = \{1 + \exp[(r - R_0)/a]\}^{-1},$$

$$q(r) = \exp\{-[(r - R_0)/b]^2\},$$

$$R_0 = r_0 A^{1/3},$$

¹¹ H. Feshbach, C. E. Porter, and V. F. Weisskopf, Phys. Rev. **96**, 448 (1954).

¹² R. D. Woods and D. S. Saxon, Phys. Rev. **95**, 577 (1954).

¹³ W. B. Riesenfeld and K. M. Watson, Phys. Rev. **102**, 1157 (1956).

¹⁴ J. R. Beyster, Los Alamos Scientific Laboratory Report LA-2099, 1957 (unpublished).

¹⁵ F. Bjorklund and S. Fernbach, Phys. Rev. **109**, 1295 (1958); University of California Radiation Laboratory Report UCRL-4927-T, 1957 (unpublished).

¹⁶ W. S. Emmerich and H. J. Amster, Bull. Am. Phys. Soc. **2**, 71 (1957).

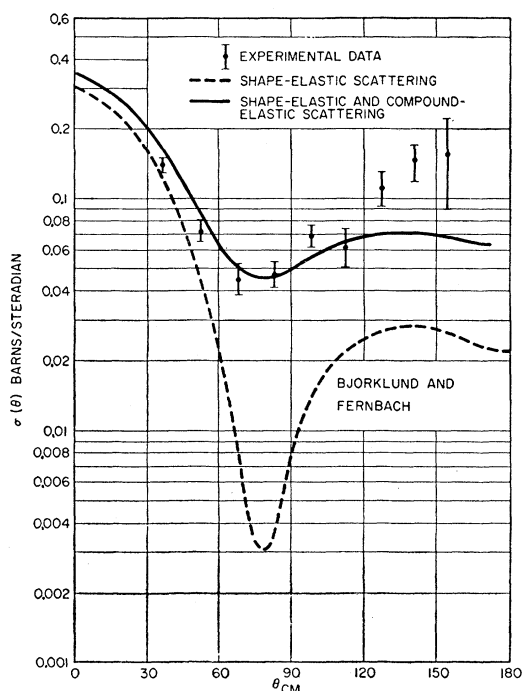


FIG. 4. Differential elastic scattering cross section for 5.6-Mev neutrons on carbon.

and V_{CR} , V_{CI} , V_{SR} , r_0 , a , and b are adjustable parameters determined from previous fits to scattering data at 4.1, 7, and 14 Mev. The values V_{CR} , V_{CI} , and V_{SR} are taken to be 47.4, 8.5, and 8.9 Mev, respectively. The values of r_0 , a , and b are 1.25, 0.65, and 0.98 fermi, respectively.

The shape-elastic scattering for carbon calculated¹⁵ using the Bjorklund-Fernbach model is shown in Fig. 4. All quantities are expressed in the center-of-mass system of coordinates. The calculations also yield values of 1.42 barns for σ_t and 0.91 barn for σ_e for carbon.

The compound-elastic scattering cannot be calculated from the theory since in the model it is assumed that

many compound nucleus states are excited at once. However, since the value of the calculated shape-elastic scattering is very small at approximately 75 degrees, a good estimate of the compound-elastic scattering may be obtained¹⁷ by taking the value of the experimental data at that angle. In this manner $\sigma_{ce}(\theta)$ is found to be approximately 0.05 barns/steradian. Assuming the same value for all scattering angles, as suggested by angular distribution data on heavy elements, the compound-elastic scattering is added to the shape-elastic scattering and the results are compared with the fully corrected experimental data in Fig. 4. The value of $\sigma_{ce}(\theta)$ is adjusted slightly to give the best over-all fit to the data.

The optical-model assumption, that the density of nuclear states in the compound nucleus is very large, is not valid for the present case. In fact, the compound levels in C^{13} around 10 Mev can be identified individually; the model does not apply to this case even in principle. The best one can hope for¹⁷ is that the model gives the average cross section for an energy range large enough to include a statistically significant number of levels in C^{13} . Any lack of agreement between experimental data and the theoretical calculation is therefore not too surprising.

ACKNOWLEDGMENT

The authors gratefully acknowledge the assistance of the staff of the Nuclear Physics and Engineering Section of the Lockheed Missile Systems Division, Palo Alto, California during the experimental work. In particular, thanks are due M. Walt, R. G. Johnson, R. D. Moffat, and F. S. Mozer for many valuable discussions and suggestions. We are indebted to F. E. Bjorklund and W. S. Emmerich for providing theoretical calculations with which to compare the experimental data. It is a pleasure to acknowledge the financial support provided by the Scientific Research Laboratory, Convair, San Diego.

¹⁷ W. S. Emmerich (private communication).